PAPER 38 (SESSION III)

# Evidence of Griffith-Orowan type intercrystalline creep fracture

R. SÖDERBERG
AB Atomenergi, 100 72 STOCKHOLM 43, Sweden

**Summary**

Intercrystalline wedge-shaped microcracks were produced in an austenitic 20% Cr-35% Ni steel by slow tensile testing at 700°C. The final fracture was made by fast tensile testing at the same temperature. In the slow tensile test a steady-state stress of about 20 kgf/mm² was attained. In the fast tensile test the material yielded at 28 kgf/mm². Specimens containing cracks above a certain length failed before the yield point was reached, with no general plastic deformation. The fracture was intercrystalline and the propagation was very fast. The relation between crack density $\nu$ and fracture stress $\sigma$ was found to obey the equation $\sigma = (\text{const.}/\log\nu)$. Determination of the largest crack at different crack densities suggested a relation $\sqrt{c} = (\text{const.}/\log\nu)$, which gives the Griffith relation $\sigma = (\text{const.}/\sqrt{c})$. In specimens fractured in the slow tensile test at 20 kgf/mm² a fast fracture started at a value of the crack density $\nu$ which satisfied the relation $\sigma = (\text{const.}/\log\nu)$ from the fast tensile test. This suggests that the fracture in the slow tensile test, which is representative of the normal creep fracture, also follows the Griffith-Orowan fracture criterion.

## Introduction and experimental method

An indication that the final fracture in intercrystalline creep fracture follows the Griffith-Orowan criterion has been found by Taplin [1]. With an approximate knowledge of fracture stress and crack length he calculated the fracture toughness of $\alpha$-brass and found a reasonable value.

In this investigation the final intercrystalline creep fracture of an austenitic steel with 20% Cr and 35% Ni was examined. The complete analysis of the steel was (per cent):

| *C* | *N* | *Si* | *Mn* | *P* | *S* | *Cr* | *Ni* |
|---|---|---|---|---|---|---|---|
| ·047 | ·03 | ·46 | ·53 | ·008 | ·008 | 18·7 | 34·4 |

The material was annealed at 1050°C to dissolve any carbides and quenched in water. The grain size was 50 $\mu$m according to the linear intercept method. The test pieces were 50 mm long and 5 mm in diameter.

The experimental method consisted of two steps. Intercrystalline wedge-shaped microcracks were first produced by slow tensile testing at 700°C. The final fracture was then effected by fast tensile testing at the same temperature. A few specimens were also fractured by slow tensile testing for comparison.

The strain rate in the slow tensile test was $1{\cdot}0.10^{-5}$ sec$^{-1}$. After some elongation a constant stress of 20 kgf/mm² was attained. The strain rate

in the fast tensile test (in a pneumatic tensile testing machine type Nemlab) was $5.10^1$ sec$^{-1}$. The yield point in the fast tensile test was reached at about 28 kgf/mm$^2$. The tensile test curve from the fast tensile test was recorded with an oscilloscope.

One object of the investigation was to examine the propagation of cracks within the elastic range between 20 and 28 kgf/mm$^2$, i.e. the possible reference of a fast fracture with no general plastic deformation. The other object was to study the relation between fracture stress and crack length.

The relation between fracture stress and crack length was studied by an indirect method. As will be shown below, the square root of the longest crack in the specimen is proportional to the logarithm of the crack density. The crack density can be determined directly from the tensile test curve by a method described in the next section. By use of this method specimens with different predetermined crack densities were produced by slow tensile testing and fractured by fast testing, and from this the fracture stress-crack length relation was analysed.

**Method for determining the fracture stress-crack density relation**

In the slow tensile test a great number of microcracks of different lengths are formed all over the specimen. They reduce the load-carrying capacity of the specimen and may be regarded as an effective crack area $\Delta A$ defined by the expression $\sigma = (F/A - \Delta A)$, $F$ being the load on the specimen, $A$ the geometrical cross-sectional area and $\sigma$ the true stress.

The determination of the quantity $\Delta A$ is illustrated in Fig. 1. After some elongation a constant stress $\sigma$ is attained. After some further elongation, however, this stress starts to decrease. It is now assumed that the true stress is constant all the time, the decrease in nominal stress being due to cracking. The relation $(\Delta\sigma/\sigma) = (\Delta A/A)$ should then be valid.

The assumption above presupposes that no recrystallisation or change in recovery rate occurs, and also that the internal cracking in fact starts at the point of decrease in stress. The latter has been checked by crack counting at different amounts of elongation and has been found to be true. No recrystallisation has been detected. It has also been proved, by measurements of the creep rate in relaxation tests in which the creep rate is determined by the true stress, that the true stress remains constant [2]. Lagneborg [3] achieved the same result from considerations of dislocation theory.

It is now obvious that there must be a connection between the crack density in the specimen and the quotient $\Delta A/A$, called the crack area. To study this relation, the crack density $\nu$ has been determined for some different values of $\Delta A/A$ by counting the cracks in sections of the specimens under a light microscope. The crack density was determined as the total crack length per 100 mm$^2$ area of section. The crack length was measured





in the number of grain boundary facets of which the crack consisted. Practically all the cracks found had stopped at triple junctions, so that the shortest cracks were of unit length and the others multiples of unit length. This method was introduced by Lindborg [4]. A total area of section of 200 mm$^2$ was investigated per specimen. The results are given in the table below. $k$ is the quotient $\nu/(\Delta A/A)$, where $\Delta A/A$ is given in per cent. The results show that there is a direct proportionality between the crack density $\nu$ and the value $\Delta A/A$.

| $\Delta A/A$ | $\nu$ | $k$ |
|---|---|---|
| 9·0 | 414 | 46·0 |
| 13·0 | 635 | 48·8 |
| 17·0 | 740 | 43·5 |
| 20·0 | 940 | 47·2 |

Lindborg [4] has proved by careful measurements that the *average* crack length is constant. He used the same alloy and the same slow hot tensile testing as in this investigation. As the average crack length $\bar{c}$ is given by $\bar{c} = (\nu/n)$, where $\nu$ is the total crack length and $n$ the number of cracks (per 100 mm$^2$), it follows that $\Delta A/A$ is directly proportional also to the number of cracks in the specimen.

**Relaxation between crack density and maximum crack length**

As an attempt to determine the possible relation between crack density and *maximum* crack length some experimental results by Lindborg [4] were examined. In the same investigation as referred to above he also determined the distribution of intercrystalline microcracks of different crack lengths. The distribution was virtually independent of the crack density but to some extent dependent upon the strain rate (stress level). By plotting Lindborg's data in a $\log X$ vs $\sqrt{c}$ diagram the distribution function was found to follow the equation $\log X = \text{const.}_1 + \text{const.}_2\sqrt{c}$, see Fig. 2. Now the fraction $X$ of crack size c also gives the probability $p(c)$ of an arbitrary crack having the length c. The probability $p(c)$ can thus be expressed as $\log p(c) = \text{const.}_1 - \text{const.}_2\sqrt{c}$. The necessary number of cracks $Z$ for the specimen to contain one crack of size $c_{max}$ is $p(c_{max})$. $Z = 1$. Substituting the expression for $p(c)$, gives after transformation $\sqrt{c_{max}} = \text{const.}_3 \log Z + \text{const.}_4$. As the number of cracks in the specimen is proportional to $\Delta A/A$, the latter relation can be written $\sqrt{c_{max}} = \text{const.}_5 \log(\Delta A/A) + \text{const.}_6$. This is the relation looked for between maximum crack length and crack density.

An experimental test of this relation was made by determining the maximum crack length for different values of $\Delta A/A$ as described above. The maximum crack lengths were plotted against $\Delta A/A$ in a $\sqrt{c}$ vs $\log(\Delta A/A)$ diagram, see Fig. No. 3. The values formed a straight line and thus confirmed the result of the analysis. If $\Delta A/A$ is expressed in per cent, as will be done in the following, the axis intercept is approximately zero and the

relation can be written $\sqrt{c}_{max}$ = const. log $\Delta A/A$. The constant is no doubt dependent upon the strain rate, since the crack distribution determined by Lindborg depended upon the strain rate. For this reason the same strain rate, $1.0 \cdot 10^{-5}$ sec$^{-1}$, was used in all slow tensile tests in this investigation.

**Results from tensile testing to fracture**

In the fast tensile test, specimens with crack areas above about 15 per cent fractured before the yield stress was reached. The maximum crack length at this crack area was determined by light microscopy as about 0·3 mm. The mode of fracture was intercrystalline, and the fracture surface formed an angle of 90° to the stress axis. The fracture took place within a time interval of $10^{-4}$ sec. This is equal to an average crack propagation speed of about 50 m/s. As the acceleration period is included in that figure, the final propagation speed must be higher. Specimens with smaller crack areas fractured above the yield point. As the crack area diminished, the elongation to fracture increased. At elongations of 1-2% the fracture was still intercrystalline. At larger elongations, however, the fracture changed to transcrystalline and formed an angle of 45° to the stress axis. The original wedge-shaped microcracks were rounded by the plastic deformation. This might be the reason why they did not propagate.

The fracture stresses from the *intercrystalline* fractures have been plotted against $\Delta A/A$ in a

$$\sigma \text{ vs } \frac{1}{\log \frac{\Delta A}{A}} \text{ diagram (see Fig. 4).}$$

The points fall on a straight line, the maximum divergences from the straight line being ± 0·5 kgf/mm² over a total investigated stress interval of 8 kgf/mm². The fracture stresses were calculated from the expression

$$\sigma = \frac{F}{A - \Delta A}.$$

The two lower points in the diagram were obtained with specimens fractured in the slow tensile test at a stress of about 20·5 kgf/mm². The crack area increased in accordance with Fig. 1. Suddenly, at a well defined value of $\Delta A/A$, the fast crack propagation started and the fracture occurred. The fracture surface formed 90° to the stress axis also in this case, and there was no sign of a contraction.

**Discussion and conclusions**

In cases of sufficiently long microcracks developed during creep a fast intercrystalline fracture occurred in the subsequent fast tensile test before





the yield point was reached. The fracture was thus a matter of unstable crack propagation. The points from the fast tensile tests form a straight line in the

$$\sigma \text{ vs } \frac{1}{\log \frac{\Delta A}{A}} \text{ diagram,}$$

which can be extrapolated to the origin. The equation for the straight line can thus be written

$$\sigma = \frac{\text{const.}}{\log \frac{\Delta A}{A}}.$$

As it has been shown that the relation $\sqrt{c}_{max}$ = const. . log $(\Delta A/A)$ is valid, the Griffith equation $\sigma = (\text{const.}/\sqrt{c})$ is obtained by substitution, if it is presupposed that the longest crack determines the fracture. The fact that straight line extrapolates to the origin means that the condition zero fracture stress at infinite crack length is fulfilled.

The conclusion from the above must be that the intercrystalline fracture in the fast tensile test follows the Griffith-Orowan fracture criterion. The question is now whether this result also holds for the intercrystalline fracture in the slow tensile test, where the conditions resemble those of normal creep. The $\sigma/(\Delta A/A)$ points from the fracture in the slow tensile tests fall on the same straight line in the

$$\sigma \text{ vs } \frac{1}{\log \frac{\Delta A}{A}} \text{ diagram}$$

as the points from the fast tensile test. This indicates that the Griffith-Orowan relation $\sigma \sqrt{c}$ = const. also holds for the fracture in the slow tensile test and for the normal intercrystalline creep fracture.

**Acknowledgement**

This paper is published by permission of AB Atomenergi. I thank Mr R. Attermo and Drs. R. Lagneborg, U. Lindborg and G. Östberg for discussions and comments as well as Avesta Jernverks AB for the use of their tensile test machine.

**References**

1. TAPLIN, D. M. R. 'A note on the relationship between cavitation and ductility'. *J. Australian Inst. Met.*, vol. 10, no. 4, pp. 336-339, 1965.
2. SÖDERBERG, R. AB Atomenergi, Stockholm 43, Work in progress, 1968.
3. LAGNEBORG, R. 'Dislocation density and dislocation arrangement during creep of 20% Cr-35% Ni stainless steels'. To be published in *Met. Sci. J.*
4. LINDBORG, U. 'Nucleation and growth of creep cracks in an austenitic steel'. To be published in *Acta Met.*

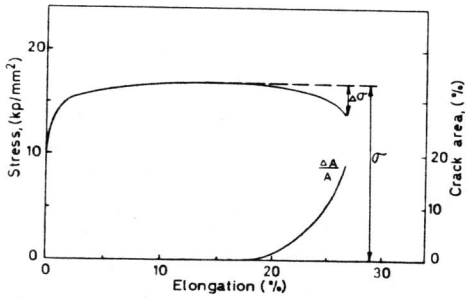


Fig. 1. Method of obtaining $\Delta A/A$ from tensile test curve. $\Delta A/A$ is given by the expression $(\Delta A/A) = (\Delta\sigma/\Delta)_\varepsilon$.

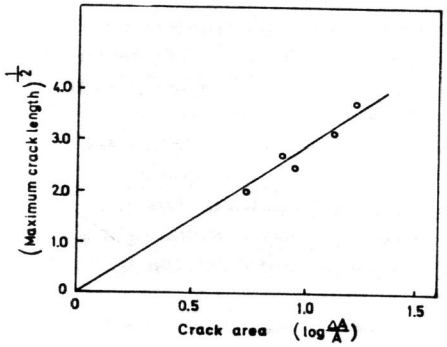


Fig. 3. Relation between maximum crack length and crack density. The crack length is measured in number of grain boundary facets. The crack density is determined as the value of $\Delta A/A$, measured in per cent.

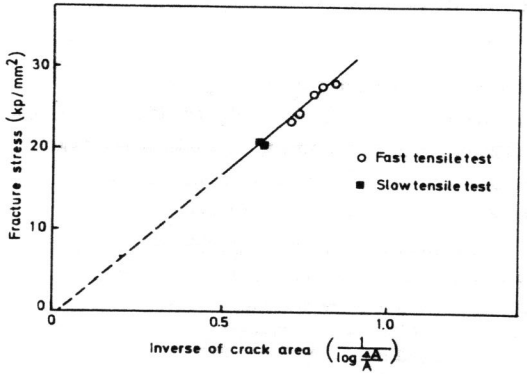


Fig. 4. Relation fracture stress-crack density. $\Delta A/A$ is measured in per cent.

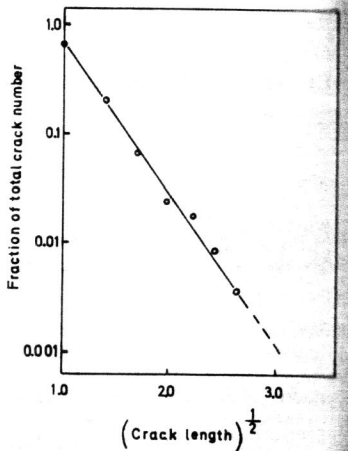


Fig. 2. Crack length distribution plotted in a log $X$ vs. $\sqrt{c}$ diagram from Lindborg's (4) experimental values. $X$ is the fraction of cracks of a particular length c. The crack length was measured around the number of grain boundary facets which it passed.

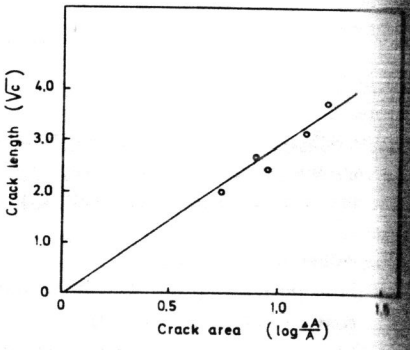


Fig. 5.





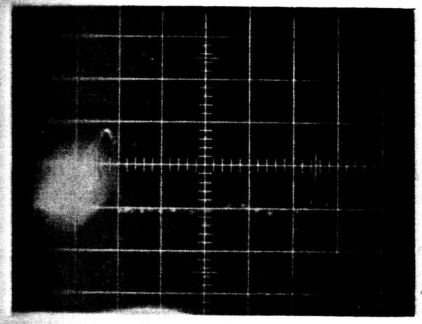

Fig. 6.

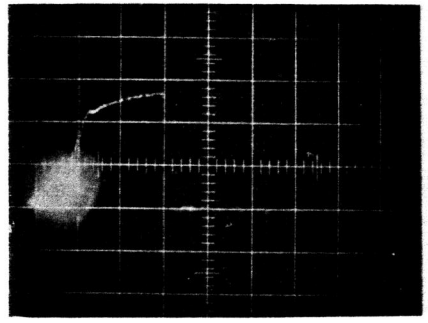

Fig. 7.

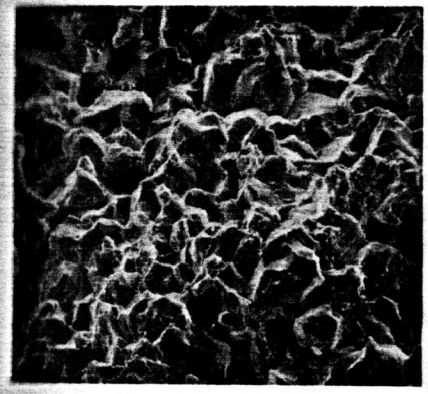

Fig. 8.

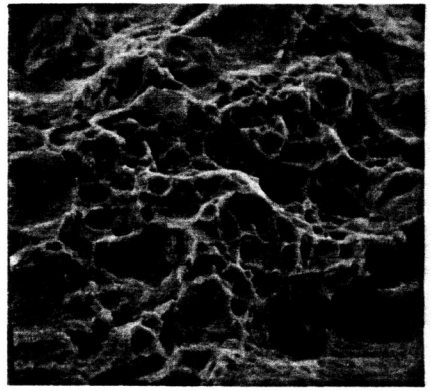

Fig. 9.

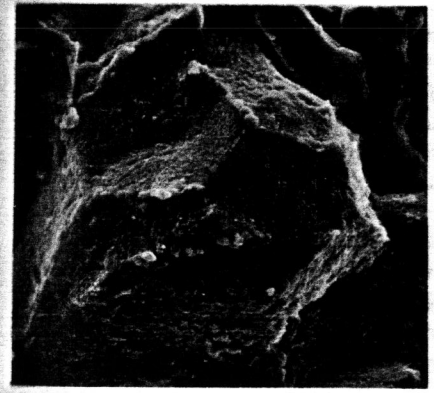

Fig. 10.

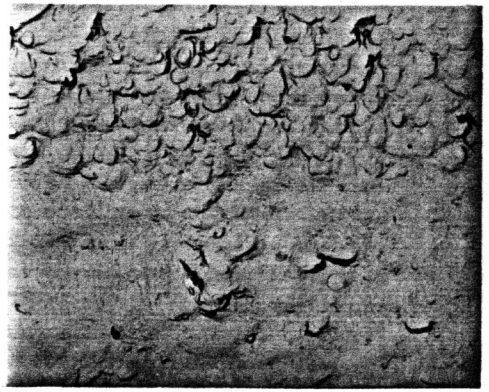

Fig. 11.